# $PdGeS_3$—A Novel One-Dimensional Metathiogermanate

**Dirk Johrendt* and Markus Tampier**

*In memory of Jean Rouxel*

**Abstract:** The novel compound $PdGeS_3$ has been synthesized by direct reaction of the elements at 600 °C. Single crystals of the fibrous material were grown in a molten flux of NaSCN. The crystal structure was determined by single-crystal X-ray diffraction techniques. $PdGeS_3$ crystallizes in the monoclinic space group $C2/m$ ($a = 14.217(6)$, $b = 3.453(2)$, $c = 9.079(6)$ Å, $\beta = 106.58(4)^\circ$, $Z = 4$). The structure is characterized by one-dimensional $^1_\infty[(PdGeS_3)_2]$ double strands that run along the $b$ axis. These are built up by two opposite chains of corner-sharing $GeS_4$ tetrahedra, representing $\{\boldsymbol{uB},\ 1^1_\infty\}[^1GeS_3]^{2-}$ einer single chains. The palladium atoms connecting these chains reside in distorted square-planar environments surrounded by four sulfur atoms. High anisotropy of chemical bonding emerged because interactions between the strands consisist of van der Waals forces exclusively. The juxtaposition of the double chains is similar to a two-dimensional hexagonal close-packed arrangement. The electronic structure and bonding is analyzed in real space by means of the electron localization function (ELF) resulting from self-consistent LMTO band structure calculations. Peculiarities in the atomic arrangement of the strands are explained by the spatial requirements of the lone pairs of electrons on sulfur and their interactions with the palladium atoms. The mutual dependencies of the bonding within and between the chains are discussed by using a two-dimensional ELF map.

**Keywords:** chalcogens · electronic structure · germanium · palladium · solid-state structures

## Introduction

Thiogermanate compounds are built up of $GeS_4$ tetrahedra separated and charge-balanced by main group or transition metal ions. In a formal sense these materials represent higher homologues of silicates. Indeed some similarities originate from the same underlying tetrahedral pattern, but silicate and thiogermanate chemistry is different and the overlap is rather limited. The reason for this is the difference in the bonds: Si – O bonds are highly ionic, whereas Ge – S bonds are almost purely covalent. Main group and transition metal thiogermanates have been known for more than 25 years. Surveys given by Olivier-Fourcade et al.[1] and Krebs[2] show a remarkable variety of structures. Many structural motifs emerge by arranging and connecting $GeS_4$ tetrahedra in various manners and combining them with the coordination polyhedra of the metal components.

Some orthothiogermanates $A_2GeS_4$ adopt structures well known from silicates like the olivine type ($A$ = Fe, Mn, Mg, Ca) with octahedral metal coordination.[3,4] With increasing ionic radii of $A^{2+}$, variants of the $K_2SO_4$ type ($A$ = Ba),[5] or special structure types ($A$ = Sr, Eu)[6] not known from silicates are formed. Unusual structures were also found for compounds with monovalent base metals such as $Tl_4GeS_4$[7] or $Li_4GeS_4$,[8] and the trivalent lanthanides $A_4Ge_3S_{12}$ ($A$ = lanthanoid).[9]

During the last few years, numerous new multinary chalcogenides have been prepared by using the reactive flux method evolved by Kanatzidis and co-workers.[10] Within this exploratory synthetic route, also new thiogermanate compounds such as $KGaGeS_4$,[11] $La_6MgGe_2S_{14}$,[12] or $KAGeS_4$ (A = lanthanoid)[13] with isolated $GeS_4$ tetrahedra were reported.

Metathiogermanates $AGeS_3$ or $A_2GeS_3$ with corner-sharing $(GeS_3)^{2n-}_n$ chains, such as $SnGeS_3$ or $Na_2GeS_3$, likewise form their own structure types.[14, 15] Analogous copper and silver compounds crystallize in blende or wurtzite-type variants with tetrahedral metal coordination.[16, 17] A common feature of all known metathiogermanates is the connection of the different $(GeS_3)^{2n-}_n$ chains by the metals. The sulfur atoms coordinating the metal never all originate from the same strand. Thus, all metathiogermanates described so far have three-dimensional structures.

The evident structural flexibility of germanium chalcogenides facilitates a tuning of their physical properties by the substitution of the metal components. These materials possess a variety of properties suitable for applications in new

[*] Dr. D. Johrendt, M. Tampier
Institut für Anorganische Chemie und Strukturchemie II
der Heinrich-Heine-Universität
Universitätsstrasse 1, D-40225 Düsseldorf (Germany)
Fax: (+49) 221-81-4146
E-mail: johrendt@uni-duesseldorf.de

  0947-6539/98/0409-1829 $ 17.50+.25/0 

technologies, such as nonlinear optics (NLO) and electro-optical devices.[18, 19] No known compound satisfies the long wish list of properties for optical materials, which is, moreover, different for each application. Thus, a deeper insight into the electronic structure of complex chalcogenides is highly recommended. Up to now no detailed description of chemical bonding in this kind of materials is available.

As mentioned above, the coordination preferences of the metal components are important factors that determine the structures of thiogermanate compounds. For this reason, we were interested in introducing transition metal atoms that exhibit coordination modes other than octahedral (like Fe) or tetrahedral (like Cu). Those metals, which prefer environments of lower dimensionality such as the nickel triade elements are expected to form a range of interesting structures when combined with different $GeS_4$ tetrahedra patterns. We chose palladium, which is expected to reside in a square-planar environment surrounded by sulfur, as a starting point for our investigations. Herein we report the synthesis, crystal structure determination, and chemical bonding of the first palladium thiogermanate $PdGeS_3$.

## Results and Discussion

The new compound $PdGeS_3$ was obtained as orange transparent fibers of up to a few millimeters in length. As seen from the scanning electron micrograph in Figure 1, the fiber diameters are less than 1 μ. Tufts are formed by accumulation of the flexible strands. Needlelike crystals, grown in a NaSCN flux were of waxlike consistency. This manifestation of the material is already indicative of the distinct one-dimensional character of the compound, which was confirmed by the structure determination.

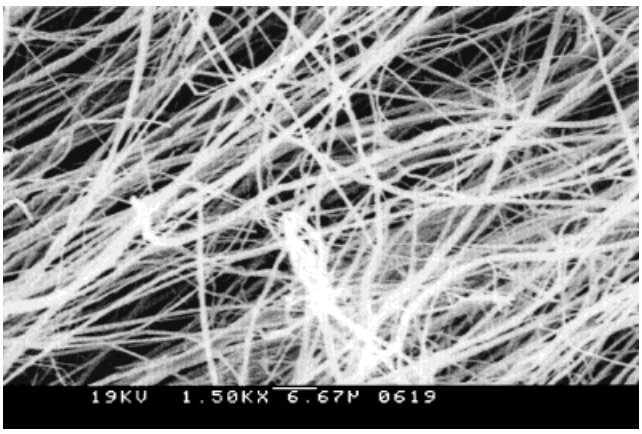


Figure 1. Scanning electron micrograph of $PdGeS_3$ fibers, magnification 1500 × .

A perspective view of the crystal structure of $PdGeS_3$ along the crystallographic *b* axis is shown in Figure 2. Selected interatomic distances and angles are compiled in Table 1. One of the main features of this novel structure type are linear one-dimensional $^1_\infty[(GeS_3)^{2-}]$ tetrahedra chains that run parallel to the *b* axis. Palladium atoms in a distorted square-planar environment surrounded by four sulfur atoms connect two adjacent chains. Two sulfur atoms come from each of the opposite chains. The Pd – S distances of 2.337 Å and 2.342 Å

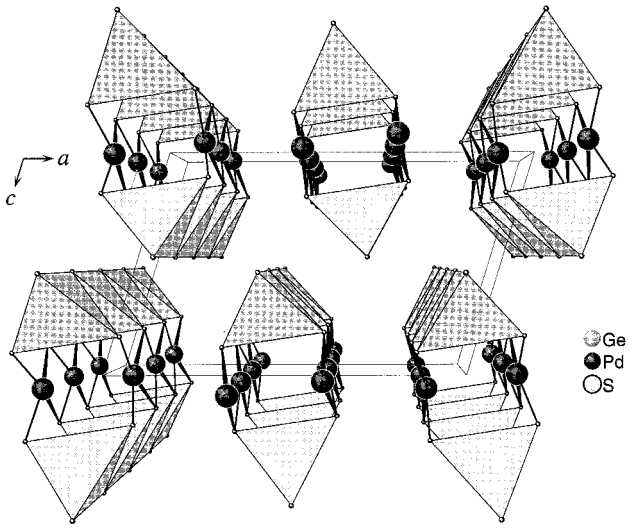


Figure 2. Crystal structure of $PdGeS_3$, perspective view along [010].

Table 1. Selected bond lengths [Å] and angles [°] of $PdGeS_3$.

| | | | |
|---|---|---|---|
| Pd – S3 | 2.337(2) × 2 | S2-Pd-S3 | 169.6(1) |
| Pd – S2 | 2.342(2) × 2 | S3-Pd-S3 | 95.3(1) |
| Pd – S2 | 3.448(3) | S2-Pd-S2 | 95.0(1) |
| Pd – Pd | 3.391(2) | S1-Ge-S1 | 101.7(1) |
| Ge – S1 | 2.226(2) × 2 | S2-Ge-S1 | 109.2(1) × 2 |
| Ge – S2 | 2.229(3) | S3-Ge-S1 | 109.0(1) × 2 |
| Ge – S3 | 2.236(3) | S2-Ge-S3 | 117.5(1) |

**Abstract in German:** *Das neuartige Metathiogermanat $PdGeS_3$ wurde durch Erhitzen der Elemente auf 600 °C dargestellt. Es bilden sich extrem dünne, orangefarbene Fasern ($\varnothing \approx 1\mu$). Einkristalle für die röntgenographische Strukturbestimmung konnten durch tempern in einer NaSCN-Schmelze erhalten werden. Hauptmerkmal der Struktur von $PdGeS_3$ (C2/m, $a = 14.217(6)$, $b = 3.453(2)$, $c = 9.079(6)$ Å, $\beta = 106.58(4)°$, $Z = 4$) sind quasi-eindimensionale $^1_\infty[(PdGeS_3)_2]$ Doppelstränge, die entlang der b-Achse verlaufen. Sie sind aufgebaut aus zwei parallelen linearen Ketten kantenverknüpfter $GeS_4$-Tetraeder. Verbunden werden je zwei dieser $\{\mathbf{uB}, 1^1_\infty\}[^1GeS_3]^{2-}$ Einer-Einfachketten durch Pd-Atome, die quadratisch-planar von S-Atomen koordiniert sind. Zwischen den Doppelsträngen wirken nur schwache van der Waals-Kräfte, die zu den extrem anisotropen mechanischen Eigenschaften führen. In der Ebene senkrecht zur Faserrichtung ähnelt die Anordnung der Stränge einer zweidimensionalen hexagonaldichten Packung. Die elektronische Struktur von $PdGeS_3$ wird mit Realraum-Techniken analysiert. Die Elektronenlokalisierungsfunktion ELF zeigt, daß Verzerrungen der Doppelstränge auf den Raumbedarf der freien Elektronenpaare des Schwefels und deren Wechselwirkungen mit den Pd-Orbitalen zurückzuführen sind. Relationen der chemischen Bindung innerhalb und zwischen den Strängen werden auf der Basis der ELF-Ergebnisse diskutiert.*



0947-6539/98/0409-1830 $ 17.50+.50/0 *Chem. Eur. J.* **1998**, *4*, No. 9

are slightly longer than that in $PdS_2$ (2.30 Å),[20] but nearly the same as that in $K_2Pd_3S_4$ (2.34 Å).[21] As seen from the S2-Pd-S3 angle of 169.6°, the palladium atoms are displaced from the square plane towards the interior of the strands. The Pd–Pd distance is 3.39 Å, that is significant longer than the Pd–Pd contacts of 3.05–3.24 Å in ternary chalcogenides $A_2Pd_3Q_4$ ($A$ = K, Rb, Cs, $Q$ = S, Se).[22]

The $GeS_4$ tetrahedra in $PdGeS_3$ are slightly distorted; Ge-S distances to the terminal sulfur atoms (Ge–S2: 2.229; Ge–S3: 2.236 Å) are longer than to the bridging sulfur (Ge–S1: 2.226 Å). This is contrary to what has so far been found in metathiogermanates such as $PbGeS_3$ and $Na_2GeS_3$, which display shorter bonds to the terminal sulfur atoms.[1] Silicates show the same behavior. Using the nomenclature for silicates derived by Liebau,[23] $PdGeS_3$ contains linear $\{\boldsymbol{uB}, {}^1_\infty\}[{}^1GeS_3]^{2-}$ chains called einer single chains; such chains have not been observed in silicates or thiogermanates. Hitherto the only representatives with einer single chains were $CuGeO_3$[24] and $K_2CuCl_3$;[25] however, in contrast to $PdGeS_3$ these compounds have three-dimensional character. This very rare structural motif, that is a single ${}^1_\infty[(PdGeS_3)_2]$ strand, is depicted in Figure 3.

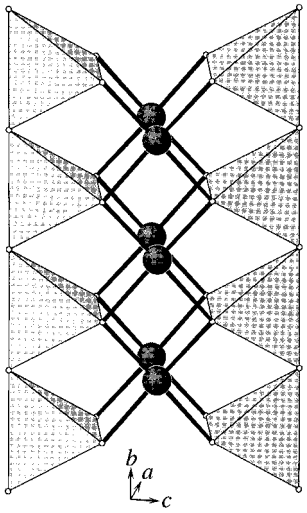


Figure 3. ${}^1_\infty[(PdGeS_3)_2]$ strand with $\{\boldsymbol{uB}, {}^1_\infty\}[{}^1GeS_3]^{2-}$ einer single chains.

Figure 4 shows a projection of the structure along the crystallographic $b$ axis. High anisotropy of chemical bonding is evident in this compound. The bonding character is covalent within the strands; however, interactions between the double chains are weak and consist of van der Waals forces exclusively. Distances between sulfur atoms of different chains of 3.45–3.7 Å are somewhat shorter than twice the van der Waals radius of sulfur (3.7 Å).[26] Weak bonding between the chains clearly explains the mechanical properties of the material, particularly the appearance of extremely fine fibers. Also the juxtaposition of the double chains in the crystal can be understood in terms of anisotropic bonding. As seen from Figure 4, six neighboring chains surround every strand in a distorted hexagonal manner. A kind of close packing results, which, however, has two restrictions: the hexagonal arrangement is distorted because of the nonspheric cross-section and the chains are at the same height (i.e. position in $y$) only along the $c$, but not along the $a$ direction due to the C-centering of the lattice. Along the $a$ axis the strands are arranged like a zip with each atom pointing towards the gaps of the neighboring chain. An evident tendency is to make the strand juxtaposition along the $b$ axis as close as possible.

A close inspection of the geometry raises questions about the distortions of the chains. At this point it is not clear why

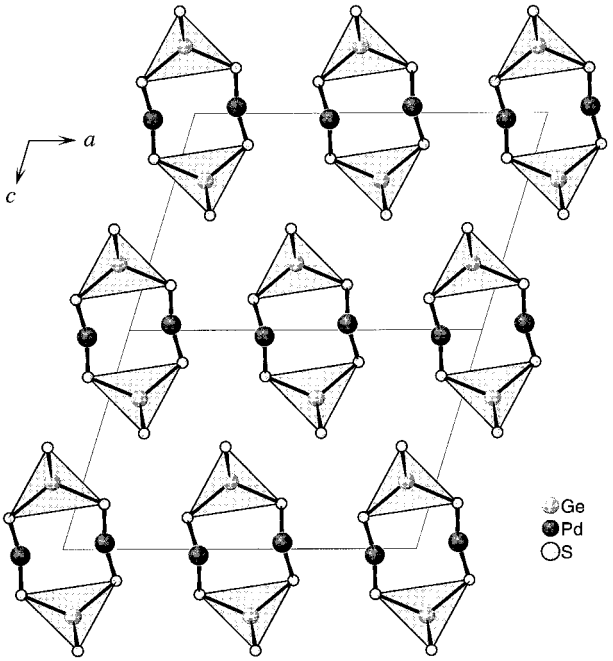


Figure 4. Crystal structure of $PdGeS_3$, projection along [010].

the distances between germanium and the two terminal sulfur atoms are different. The strands could be symmetric because of their molecular character. In particular the reason for the significant displacement of the palladium atoms from the plane of sulfur atoms is not clearly evident. More detailed information about the chemical bonding is required in order to explain these results.

To gain a better insight into the chemical bonding in $PdGeS_3$, band structure calculations were carried out with the LMTO-method. For the sake of clarity, the discussion is confined to the more vivid real space representations of the electronic structure. Figure 5 shows the total density of states and the contribution of the palladium 4d orbitals (shaded area) of $PdGeS_3$. The 3s states of sulfur and 4s states of germanium extend around $-13$ and $-8$ eV, respectively. Between $-6$ eV and the Fermi level we find the p levels of

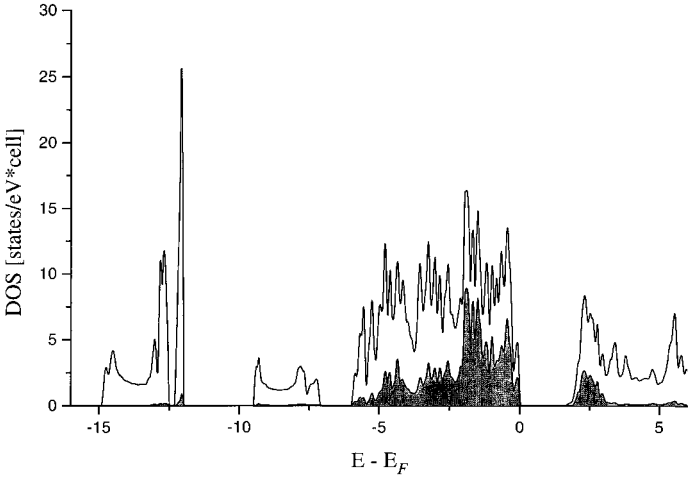


Figure 5. Electronic density of states for $PdGeS_3$; the energy zero is taken at the Fermi level.

sulfur and germanium mixed with the metal 4d states. The strong broadening of the Pd 4d levels indicates various interactions with the orbitals of the neighboring atoms. As expected from the charge-precise ionic formula splitting $Pd^{2+}Ge^{4+}(S^{2-})_3$, the material is a semiconductor. The calculated energy gap is 1.6 eV, but it must be kept in mind that the local density approximation always produces energy gaps that are much smaller than the experimental values. Above the Fermi level the palladium 4d contribution around +2.5 eV can be assigned to the $x^2 - y^2$ orbital pushed up in energy by the crystal field splitting.

The significant displacement of the Pd atoms from the square plane towards the interior of the strands leads to a Pd–Pd distance of 3.39 Å. An attractive metal–metal bonding interaction, if any exists, must be made by the Pd $4dz^2$ orbitals pointing towards the neighboring metal atom. The analysis of the band structure near the Fermi level reveals Pd-Pd ddσ* antibonding character for the $z^2$ orbitals near the top of the valence band. These antibonding states are filled; thus we conclude that no Pd–Pd bonding takes place within the chains. Reasons for the displacement out of the plane may rather be found in the juxtaposition of the strands. This should be governed by the competition between the closest packing and the spatial requirements of the lone pairs on sulfur. Of course the arrangement which yields the lowest total energy will determine the structure.

Figure 6 shows the electron localization function (ELF) calculated for the (010)-plane perpendicular to the chains at $y = 0$. The shape and orientation of the lone pairs of electrons

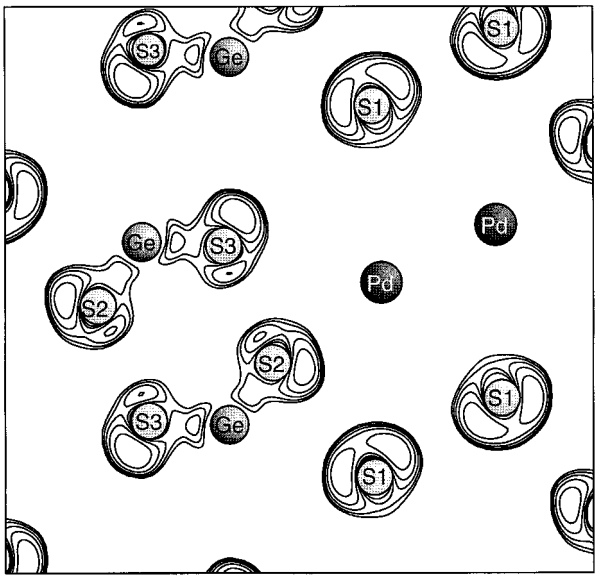


Figure 6. Electron localization function (ELF); (010)-plane at $y = 0$; contour values are 0.8 to 0.96.

on sulfur are clearly visible. High localization (ELF $\geq 0.9$) is also discerned in the bonding region between S2/S3 and Ge, as expected for covalent Ge–S bonding. Maxima at S2 pointing towards S3 and vice versa are residuals from the Pd–S bonds that lie outside the plane. Regions with high ELF values are remarkably different around the sulfur atoms S2 and S3. The lone pair of electrons at S3 points towards empty space, but less space is available around S2. A significant deformation of the lone pair topology is visible at S2 (compare with S3). As seen from the ELF topology, it avoids interaction with the neighboring palladium atom. This effect appears weak, since the Pd–S2 distance is 3.45 Å; however, the S2 atom is located above the square plane of sulfur atoms around the palladium atom, and thus, the S2 lone pair of electrons interacts with the Pd $dz^2$ orbital lobe pointing out of the chain. Both orbitals are filled, so a repulsive interaction (pdσ* antibonding) results. This situation is similar to that in $PdS_2$, where Pd adopts square-planar coordination with two additional sulfur atoms above and below the plane, leading to elongated octahedra.[20] The two longer Pd–S distances in $PdS_2$ are 3.3 Å. Clearly this repulsive interaction cannot be weak, because it changes the cubic pyrite type to the layered $PdS_2$ structure. Evidently, the same force is working in $PdGeS_3$: the electronic repulsion deforms the lone pair of electrons on S2. In order to make the Pd–S2 distance as long as possible, the Pd atoms are displaced towards the interior of the strands. At the same time the charge distribution (and thus the ELF) around S2 is reorganized compared to that around S3, leading to slightly different Pd–S and Ge–S bond lengths. As the ELF analysis shows, the weak asymmetry of the terminal Ge–S bonds and the shift of the Pd atoms indeed have their origin in the special juxtaposition of the one-dimensional chains. Antibonding interactions between Pd and the lone pair of electrons on S2 distort the strands, but nevertheless this is the arrangement of lowest energy in the solid state.

## Experimental Section

**General Remarks**: Starting materials were palladium metal powder (Degussa, 99.99 %), germanium powder (Chempur, 99.999 %), and S flakes (Chempur, 99.999 %).

**Palladium metathiogermanate, $PdGeS_3$**: A stochiometric mixture of Pd powder (0.232 g, 2.18 mmol), Ge (0.1583 g, 2.18 mmol), and S flakes (0.2097 g, 6.54 mmol) was loaded into a silica tube. After the tube had been evacuated and flushed with argon three times, it was sealed under an argon atmosphere (ambient pressure). The mixture was heated at a rate of $50\,^{\circ}C\,h^{-1}$ to 600 °C, kept at this temperature for one week, and then the furnace was allowed to cool to room temperature. This procedure produced tufts of extremely fine transparent orange fibers (diameter $\leq 1$ μ, length up to 1 mm) of $PdGeS_3$, which are stable in air and insoluble in water, $CS_2$, and common organic solvents. In order to grow crystals, the product was annealed in a molten flux of NaSCN at 600 °C for one week. NaSCN was vacuum-dried at 120 °C before use. After the flux had been dissolved in water and dried in vacuum, orange needlelike crystals were obtained. No impurities could be detected within the accuracy of the X-ray powder diffraction experiment, although traces of binary palladium sulfides were visible in the microscope.

**Structure determination**: The crystal structure was determined by single-crystal X-ray diffraction at room temperature. A Siemens P3 diffractometer was used for the data collection. Lorentz and polarization corrections were performed. Small absorption effects remained uncorrected. The structure was solved in the space group *C2/m* by using direct methods (SHELXTL)[27] and refined against $F_o^2$ (SHELXL-93),[28] Final refinements included anisotropic displacement parameters for all atoms. Details of the data collection and refinement are given in Table 2; the final atomic and equivalent displacement parameters are listed in Table 3. Important



0947-6539/98/0409-1832 $ 17.50+.50/0 *Chem. Eur. J.* **1998**, *4*, No. 9

Table 2. Crystal data and details of the data collection of $PdGeS_3$.

| | |
|---|---|
| empirical formula | $PdGeS_3$ |
| formula weight | 275.17 |
| diffractometer | Siemens P3 |
| radiation, wavelength [Å] | $Mo_{K\alpha}$, $\lambda = 0.71073$ |
| monochromator | graphite |
| data collection mode | $\theta$-$2\theta$ scan |
| crystal size [mm] | $0.02 \times 0.25 \times 0.02$ |
| T [K] | 298 |
| crystal system | monoclinic |
| space group | *C2/m* |
| *a* [Å] | 14.217(6) |
| *b* [Å] | 3.453(2) |
| *c* [Å] | 9.079(6) |
| $\beta$ [°] | 106.58(4) |
| *V* [Å$^3$] | 427.1(8) |
| *Z* | 4 |
| $\rho_{calcd}$ [g cm$^{-3}$] | 4.298 |
| $\mu$ ($Mo_{K\alpha}$) [mm$^{-1}$] | 12.54 |
| $\theta$-range [°] | 3–35 |
| data collected | 2709 |
| unique data | 1076 ($R_{int} = 0.106$) |
| refinement method | full-matrix, based on $F^2$ |
| parameters | 32 |
| $R_1(F > 4\sigma(F))$, $R_1$(all) | 0.058, 0.091 |
| $wR_2$ (all) | 0.156 |
| goodness-of-fit | 0.931 |
| largest diff. peak/hole [e Å$^{-3}$] | 2.82/ − 2.14 |

Table 3. Atomic coordinates and equivalent displacement parameters for $PdGeS_3$ (all atoms in 4*i* (*x*,*0*,*z*), standard deviations in parentheses).[a]

| Atom | *x* | *z* | $U_{eq}$[a] |
|---|---|---|---|
| Pd | 0.3873(1) | 0.0286(1) | 0.0164(2) |
| Ge | 0.0861(1) | 0.3091(1) | 0.0170(2) |
| S1 | 0.6294(2) | 0.4689(3) | 0.0200(5) |
| S2 | 0.1768(2) | 0.1453(3) | 0.0191(5) |
| S3 | 0.9229(2) | 0.2095(3) | 0.0185(5) |

[a] The equivalent displacement parameter is defined as one-third of the orthogonalized $U_{ij}$ tensor.

interatomic distances and angles are summarized in Table 1. Further details of the crystal structure investigations can be obtained from the Fachinformationszentrum Karlsruhe, D-76344 Eggenstein-Leopoldshafen, Germany (fax: (+49) 7247-808-666; e-mail: crysdata@fiz-karlsruhe.de), on quoting the depository number CSD-408505.

**Electronic structure calculations**: Self-consistent ab initio band structure calculations were performed using the LMTO method in its scalar relativistic version (program LMTO-ASA 47).[29] A detailed description may be found elsewhere.[30–34] Reciprocal space integrations were performed with the tetrahedron method using 524 irreducible *k*-points within the Brillouin zone.[35] The basis sets consisted of 4d/5s/5p orbitals for Pd, 4s/4p for Ge and 3s/3p for S. The 3d orbitals for S, 4d for Ge, and 4f for Pd were treated by the downfolding technique.[36] To achieve space filling within the atomic sphere approximation, interstitial spheres are introduced to avoid too large overlap of the atom-centered spheres. The empty sphere positions and radii were calculated by using an automatic procedure developed by Krier et al.[37] An overlap of more than 15 % was not allowed for any two atom-centered spheres. A two-dimensional grid of the ELF[38] was calculated. Within density functional theory, ELF depends on the excess of local kinetic energy due to the Pauli principle compared with the bosonic system (Pauli kinetic energy $t_{P(r)}$). By definition the values for ELF are confined to [0,1]. Regions in space, where the Pauli principle does not increase the kinetic energy of the electrons (i.e. high values of ELF) can be identified as areas where pairing of electrons with opposite spins play an important role. Thus, high values of ELF can be treated as equivalent to covalent bonds or lone pairs of electrons.[39]

**Acknowledgments:** We are indebted to Prof. A. Mewis and Prof. D. Mootz for fruitful discussions and financial support of this work. We thank Dr. U. König for the SEM investigation.

Received: April 16, 1998 [F 1098]

[1] J. Olivier-Fourcade, J. C. Jumas, M. Ribes, E. Philippot, M. Maurin, *J. Solid State Chem.* **1978**, *23*, 155.
[2] B. Krebs, *Angew. Chem.* **1983**, *95*, 113; *Angew. Chem. Int. Ed. Engl.* **1983**, *22*, 113.
[3] H. Vincent, E. F. Bertaut, W. H. Baur, R. D. Shannon, *Acta Crystallogr. B* **1976**, *32*, 1749.
[4] Tranqui-Duc, H. Vincent, E. F. Bertaut, Vu Van Qui, *Solid State Commun.* **1969**, *7*, 641.
[5] G. Rocktäschel, W. Ritter, A. Weiss, *Z. Naturforsch. B* **1964**, *19*, 958.
[6] G. Eulenberger, D. Müller, *Z. Naturforsch. B* **1974**, *29*, 118.
[7] M. Ribes, M. Maurin, *Rev. Chim. Miner.* **1970**, *7*, 75.
[8] M. G. Kanatzidis Y. Matsushita, *Z. Naturforsch. B* **1997**, *53*, 23.
[9] A. Michelet, A. Mazurier, G. Collin, P. Laurelle, J. Flahaut, *J. Solid State Chem.* **1975**, *13*, 65.
[10] M. G. Kanatzidis, A. C. Sutorik, *Progr. Inorg. Chem.* **1995**, *43*, 151.
[11] P. Wu, Y.-J. Lu, J. A. Ibers, *J. Solid State Chem.* **1992,** *97*, 383.
[12] R. L. Gitzendammer, C. M. Spencer, F. J. DiSalvo, *J. Solid State Chem.* **1996**, *131*, 399.
[13] C. K. Bucher, S.-J. Hwu, *Inorg. Chem.* **1994**, *33*, 5831.
[14] J. Fenner, D. Mootz, *Naturwissenschaften* **1974,** *61*, 127.
[15] J. Olivier-Fourcade, E. Phillipot, M. Ribes, M. Maurin, *Rev. Chim. Miner.* **1972**, *9*, 757.
[16] E. Parthe, J. Garin, *Monatsh. Chem.* **1971**, *102*, 1197.
[17] A. Nagel, K.-J. Range, *Z. Naturforsch. B* **1978**, *33*, 1461.
[18] *Materials for Nonlinear Optics*, (Eds.: S. R. Marder, J. E. Sohn, G. D. Stucky), ACS Symposium Series, *Vol 455*, American Chemical Society, Washington D. C., **1991**.
[19] S. K. Kurtz, *IEEE J. Quant. Electronics* **1968**, *QE-4*, 578.
[20] E. Roest, F. Groenvold, *Acta Crystallogr.* **1956**, *10*, 329.
[21] J. Huster, W. Bronger, *J. Solid State Chem.* **1974**, *11*, 254.
[22] R. Rennau, D. Schmitz, W. Bronger, *Z. Anorg. Allg. Chem.* **1991**, *597*, 27.
[23] F. Liebau, *Structural Chemistry of Silicates,* Springer, Heidelberg, **1985**, p. 102
[24] C. Brink, C. H. MacGillavry, *Acta Crystallogr.* **1949**, *2*, 158.
[25] A. Wittmann, H. Nowotny H. Völlenkle, *Monatsh. Chem.* **1967**, *98*, 1353.
[26] L. Pauling, *Die Natur der chemischen Bindung,* 3rd ed., VCH, Weinheim, **1968**, p. 249.
[27] Structure Determination System SHELXTL-PLUS, Rev. 4.21/V, Siemens Analytical X-Ray Instruments Inc.; Madison, WI, USA, **1990**.
[28] G. M. Sheldrick, Crystal Structure Refinement SHELXL93, Universität Göttingen, **1993**.
[29] O. K. Andersen, Tight-Binding LMTO Vers. 47, Max-Planck-Institut für Festkörperforschung, Stuttgart, **1994**.
[30] O. K. Andersen, *Phys. Rev.* **1975**, *B12*, 3060.
[31] O. Jepsen, O. K. Andersen, *Phys. Rev. Lett.* **1984**, *53*, 2571.
[32] O. K. Andersen, O. Jepsen, *Z. Phys. B* **1995**, *97*, 35.
[33] H. L. Skriver, *The LMTO Method*, Springer, Berlin **1984**.
[34] O. Jepsen, M. Snob O. K. Andersen, *Linearized Band-Structure Methods in Electronic Band-Structure and its Applications*, Springer Lecture Notes, Springer, Berlin, **1987**.
[35] O. K. Andersen, O. Jepsen, *Solid State Comm.* **1971**, *9*, 1763.
[36] W. R. L. Lambrecht, O. K. Andersen, *Phys. Rev.* **1986**, *B34*, 2439.
[37] G. Krier, O. Jepsen, O. K. Andersen, unpublished results.
[38] A. Savin, B. Silvi, *Nature* **1994**, *371*, 683.
[39] A. Savin, T. F. Fässler, *Chem. Unserer Zeit* **1997**, *31*, 110.